RSC Advances

PAPER

View Article Online
View Journal | View Issue

Cite this: *RSC Adv.*, 2017, **7**, 49618

A stable 3D Cd(II) metal–organic framework for highly sensitive detection of Cu^{2+} ions and nitroaromatic explosives†

Jian-Long Du,*[ab] Ju-Ping Gao,[ab] Chao-Ping Li,[ab] Xiao-Ying Zhang,[ab] Jin-Xin Hou,[ab] Xu Jing,*[ad] Ya-Juan Mu[c] and Li-Jun Li[ab]

Received 14th August 2017
Accepted 19th October 2017

DOI: 10.1039/c7ra08977e

rsc.li/rsc-advances

A Cd(II) coordination polymer, $[Cd_3(L)_2(H_2O)_5]\cdot(H_2O)_4$ (**1**) (H_3L = 9-(4-carboxy-phenyl)-9*H*-carbazoly-3,6-dicarboxylic acid) has been synthesized solvothermally. Compound **1** exhibits excellent luminescence and good stability in aqueous and DMF solution. In particular, **1** can detect Cu^{2+} ions through fluorescence quenching in aqueous solution. In addition, **1** also shows a highly sensitive response to some nitroaromatic compounds (NACs) in DMF solution. Thus, **1** can serve as a promising luminescent sensor for detecting Cu^{2+} ions and NACs.

1. Introduction

Nowadays, rapid detection of metal ions and nitroaromatic compounds (NACs) has attracted much attention because of their importance for environmental safety and homeland security.[1–4] Among different metal ions, Cu^{2+} ion is one of the most essential ions in living biosystems, especially in the brain.[5] Both deficiency and overload of copper may cause some types of severe diseases, for instance hematological manifestations, Alzheimer's, and Wilson's diseases.[6] On the other hand, with the development of chemical industry all over the world, some widely used chemicals such as nitroaromatic compounds (NACs) have become a highlight research focus in recent years due to their high toxicity to the environment and human health, especially due to their easy explosivity. Therefore, the development of convenient, cost effective Cu^{2+} ions and NAC detecting methods is a very important issue.

Metal–organic frameworks (MOFs) have diversity of structures,[7–9] which have been widely applied in recent years.[10–17] Among different types of MOFs, excellent stability and specific structure endow luminescent MOFs the ability to detect metal ions (Cu^{2+}, Fe^{3+}), explosives (nitrobenzene, 4-nitrophenol, TNT, and 2,4,6-trinitrophenol), and inorganic anions (NO_3^-, Cl^-, CrO_4^{2-}).[18–28] Compared with other detailed methods, luminescent MOFs as the probes have the advantages of outstanding sensitivity, fast response, easy manipulation and cost-effective. Recently, luminescent MOFs act as chemical sensors have been reported. Cao have designed a water stable luminescent MOF, which can rapidly sensing of Fe^{3+} and Al^{3+} ions from mixed metal ions.[29] Jia have chosen a fluorescent anionic MOF sensing of Cr^{3+} ion and TNP.[30] To the best of our knowledge, luminescent MOFs act as sensors of both Cu^{2+} ion and NACs are still relatively rare.[31]

Herein, we select a tricarboxylic acid (9-(4-carboxy-phenyl)-9*H*-carbazolyl-3,6-dicarboxylic acid, H_3L) as a ligand (Scheme 1), Cd(II) ions as the metal nodes to synthesis a luminescent Cd-MOF. Choosing these materials to construct MOFs is mainly based on the following considerations: (1) H_3L ligand is a π electron-rich organic ligand with good electron-transferring ability. The carboxylate groups can take multi coordination modes to meet the coordination requirements of the metal ions; (2) Cd(II) ions have different coordination numbers and can provide multi-coordination modes, which help to construct high dimensional coordination networks; (3) MOFs built from π-

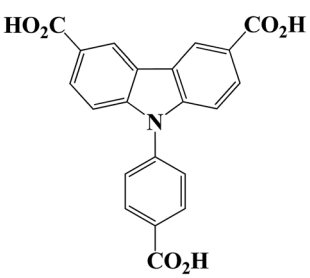

Scheme 1 Structure of H_3L

[a]College of Chemistry & Environmental Science, Chemical Biology Key Laboratory of Hebei Province, Hebei University, Baoding 071002, P. R. China. E-mail: dujl@hbu.cn; Jingxu3@126.com; Tel: +86-312-5079359

[b]Key Laboratory of Medicinal Chemistry, Molecular Diagnosis of Ministry of Education, Hebei University, Baoding 071002, P. R. China

[c]College of Traditional Chinese Medicine, Hebei University, Baoding 071000, P. R. China

[d]State Key Laboratory of Fine Chemicals, Dalian University of Technology, Dalian 116024, P. R.China

† Electronic supplementary information (ESI) available. CCDC 1556041 (for **1**). For ESI and crystallographic data in CIF or other electronic format see DOI: 10.1039/c7ra08977e

conjugated ligands and d^{10} metal ions, such as Cd^{2+} ion, are promising luminescent candidates. Therefore, a novel luminescent Cd-MOF (**1**), has been designed and synthesized using H_3**L** ligand and Cd^{2+} ion under solvothermal condition, which exhibits good stability in both aqueous and DMF solution. Compound **1** can detect Cu^{2+} ions and NACs through fluorescence quenching with high sensitivity. In addition, the possible quenching mechanisms have also been discussed.

2. Experimental

2.1 Materials and general methods

All reagents were obtained commercially and purified by standard methods prior to use. H_3**L** was synthesized by modified the literature method (Scheme S1 in the ESI†). ^{1}H NMR spectra were recorded on a Bruker Advance III 600 spectrometer medium at 25 °C with tetramethylsilane as the internal reference. The IR absorption spectra were recorded in the range of 4000–400 cm^{-1} on a Nicolet 380 FT-IR spectrophotometer with KBr pellets. Elemental analyses were performed on a CE-440 elemental analyzer. Power X-ray diffractions patterns (PXRD) were collected on a Bruker D8 ADVANCE diffractometer with Cu-Kα radiation ($\lambda = 1.5418$ Å). Thermogravimetric analysis (TGA) was performed under a nitrogen atmosphere with a heating rate of 10 °C min^{-1} using a NETZSCH STA 449C unit. Fluorescence spectra were recorded on a Hitachi F-7000 fluorescence spectrophotometer which was equipped with a xenon lamp and a quartz carrier at ambient temperature. X-ray photoelectron spectroscopy (XPS) was performed on the Thermo Scientific ESCALab 250Xi using 200 W monochromated Al Kα radiation.

2.2 Synthesis of compound 1

$[Cd_3(\mathbf{L})_2(H_2O)_5]\cdot(H_2O)_4$ A mixture of H_3**L** (3 mg, 0.008 mmol), $3CdSO_4\cdot 8H_2O$ (50 mg, 0.065 mmol) DMF (2 mL), and H_2O (3 mL), was put into a 10 mL glass vial and subsequently heated to 80 °C for 48 h, after cooled, yellow block crystals of **1** was obtained. Yield: 32%. FT-IR (KBr pellet, cm^{-1}): 3431 m, 1653 w, 1603 s, 1542 m, 1472 m, 1390 s, 1294 w, 1277 w, 781 s, 680 w, 648 w, 526 w, 487 w. Anal. calcd for $C_{42}H_{38}N_2O_{21}Cd_3$: C, 40.55; H, 3.08; N, 2.25; found: C, 40.61; H, 3.14; N, 2.19%.

2.3 Crystal structures determination

Single-crystal X-ray diffraction measurements for compound **1** was carried out on a Bruker AXS Smart APEX-II diffractometer with Mo-Kα radiation ($\lambda = 0.71073$ Å) at 293 K. Data processing was completed with the SAINT processing program.[32] The structure was solved by direct methods and refined on F^2 by full-matrix least-squares with the SHELX-97 program.[33] All non-hydrogen atoms were refined with anisotropic displacement parameters, the C19 carboxyl and its coordinated atoms of Cd4 and Cd5 were all refined with a disorder model. Hydrogen atoms were added theoretically, riding on the concerned atoms and refined with fixed thermal factors, and the hydrogen on water molecules were not located. Attempts to locate and model the highly disordered solvent molecules in the pores were unsuccessful. Therefore, the SQUEEZE routine of PLATON was used to remove the diffraction contribution from guests to produce a set of solvent-free diffraction intensities. The guest molecules can be calculated according to the TGA and elemental analyses. The crystallographic data for **1** is

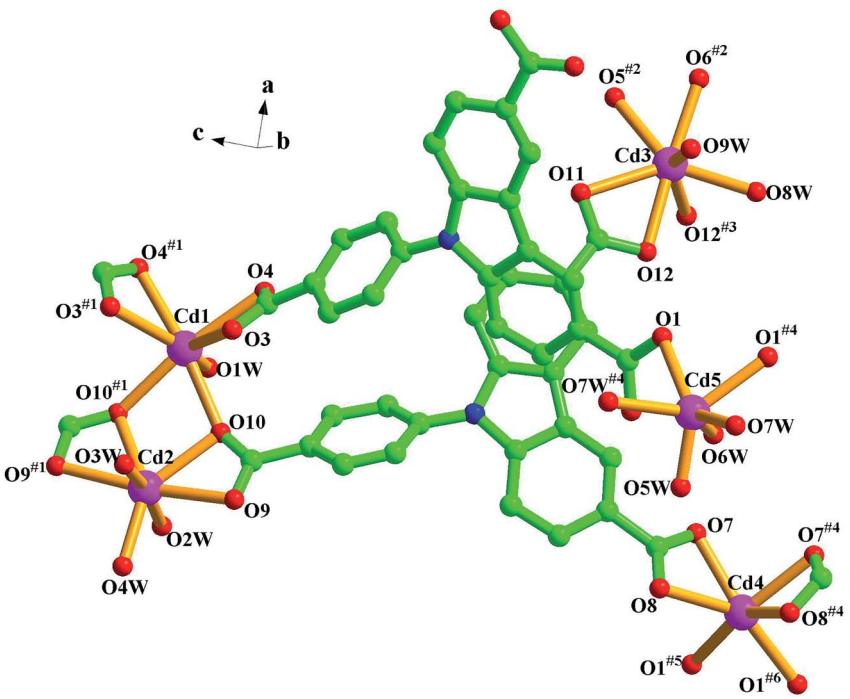

Fig. 1 View of the coordination environment of the Cd(II) ion in **1** (symmetry code: #1 *x*, *y*, −*z* + 1; #2 −*x* + 5/2, *y* + 1/2, *z*; #3 −*x* + 2, −*y* + 1, *z*; #4 *x*, *y*, −*z*; #5 *x* - 1/2, −*y* + 1/2, *z*; #6 *x* - 1/2, −*y* + 1/2, −*z*).

summarized in Table S1,† and selected bond lengths and angles are given in Table S2† of the ESI.

CCDC reference number 1556041 (for **1**).†

2.4 Luminescent measurement

For the properties of sensing with respect to various metal ions, the compound **1** (18 mg) was grinded into the powder and suspended in 18 mL aqueous solution, sonicated for 30 min to ensure even dispersion. $M(NO_3)_x$ (1×10^{-3} M; M = Na^+, K^+, Ag^+, Mg^{2+}, Co^{2+}, Ca^{2+}, Ni^{2+}, Zn^{2+}, Cd^{2+}, Mn^{2+}, Cu^{2+}, Hg^{2+}, and Cr^{3+}) was added into the aqueous suspension of compound **1** at room temperature, respectively. For the sensing of NACs, compound **1** (2 mg) was immersed in 2 mL of the different organic solvents (acetonitrile (MeCN), *N*,*N*′-dimethyl formamide (DMF), tetrahydrofuran (THF), dichloromethane (DCM), acetone (DMK), methanol (MeOH), and nitrobenzene (NB)) at room temperature, then used for luminesent measurements immediately.

3. Results and discussion

3.1 Crystal structure of $[Cd_3(L)_2(H_2O)_5]\cdot(H_2O)_4$

Single-crystal structure analysis reveals that compound **1** crystallizes in the orthorhombic system with a *Pbam* space group. The asymmetry unit contains three crystallographically independent Cd^{2+} ions, two L^{3-} ligands, five coordination water molecules, and four lattice water molecules. As illustrated in Fig. 1 and S1,† Cd1, Cd2, and Cd3 are involved in seven-coordinate sites, but the detailed environments are different. Cd1 is coordinated by six carboxylate oxygen atoms (O3, $O3^{\#1}$, O4, $O4^{\#1}$, O10, $O10^{\#1}$) from four L^{3-} ligands and one water molecule (O1W). Around Cd2, four carboxylate oxygen atoms (O9, $O9^{\#1}$, O10, $O10^{\#1}$) of two different L^{3-} ligands and three water molecules (O2W, O3W, O4W). For Cd3, seven coordinated oxygen atoms come from five carboxylate oxygen atoms ($O5^{\#2}$, $O6^{\#2}$, O11, O12, $O12^{\#3}$) in three different ligands, and two water molecules (O8W, O9W). So Cd1, Cd2 and Cd3 adopt distorted pentagonal bipyramidal geometries. While, Cd4 and Cd5 show six-coordinate modes and they are located at octahedral geometries. Around Cd4, there are six carboxylate oxygen atoms ($O1^{\#5}$, $O1^{\#6}$, O7, O8, $O7^{\#4}$, $O8^{\#4}$) from four different L^{3-} ligands, while Cd5(II) is surrounded by two oxygen atoms (O1, $O1^{\#4}$) from different L^{3-} ligands and four water molecules (O5W, O6W, O7W, $O7W^{\#4}$). And all the Cd–O bond distances between 1.86(4) and 2.480(8) Å, with O–Cd–O angles are between 53.5(3)° and 176.7(4)°.

From a topological viewpoint, every two Cd^{2+} ions (Cd1 and Cd2, Cd3 and $Cd3^{\#3}$, Cd4 and Cd5) are bridged by carboxyl groups, which form a binuclear cluster. Each cluster is linked by four L^{3-}, which can be regarded as four-connected node (Fig. 2b). And the carboxyl groups of each L^{3-} ligand are respectively linked to three binuclear clusters, therefore, each L^{3-} ligand can be considered as a three-connected node (Fig. 2a). With the linkage of ligands, the whole molecule exhibits a 3D coordination network, which can be simplified into a (3, 4, 4, 4) net with the symbol of $(4\cdot8^2)_4(4^2\cdot8^4)_2(8^4\cdot12^2)$ (Fig. 2c).

3.2 PXRD and thermal stability of 1

The PXRD patterns show that the main peaks of the synthesized MOFs are closely consistent with the simulated one, indicating the high phase purity of the samples of **1** (Fig. S2†). Thermal gravimetric analysis (TGA) of **1** was conducted under nitrogen atmosphere from 25 °C to 800 °C with a heating rate of 10 °C min^{-1}. A weight loss from 25 °C is due to the departure of five coordinated water molecules and four free water molecules (obsd 13.38%, calcd 13.02%). And the framework of **1** begins to collapse at about 380 °C, indicating that compound **1** has good thermal stability (Fig. S3†).

3.3 Luminescent properties

MOFs containing d^{10} metal ions had been attracted much attention for their potential applications as chemical sensors.[34]

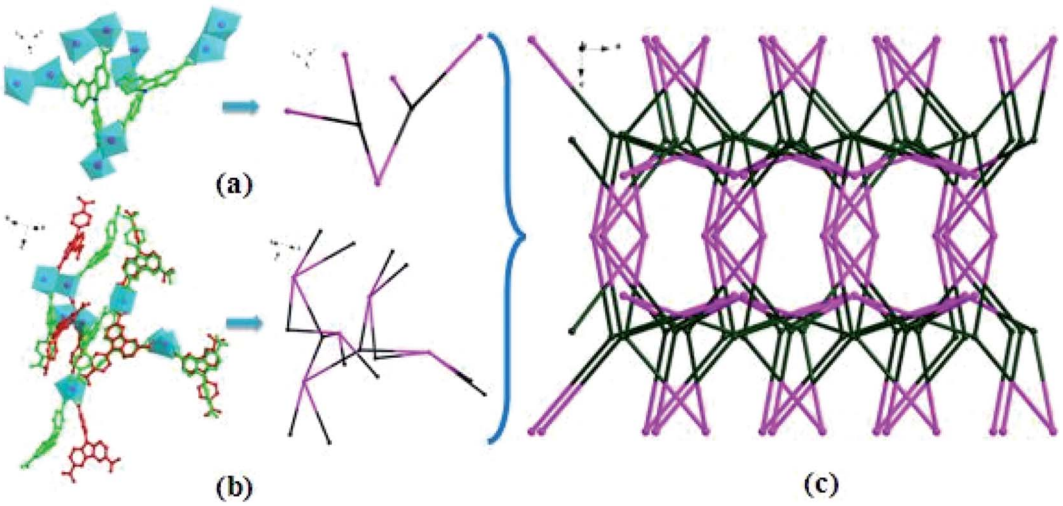

Fig. 2 View of (a) L^{3-} ligand considered as a three-connected node; (b) Cd(II) regarded as four-connected node; (c) the 3, 4, 4, 4-connected 3D topology of **1**.

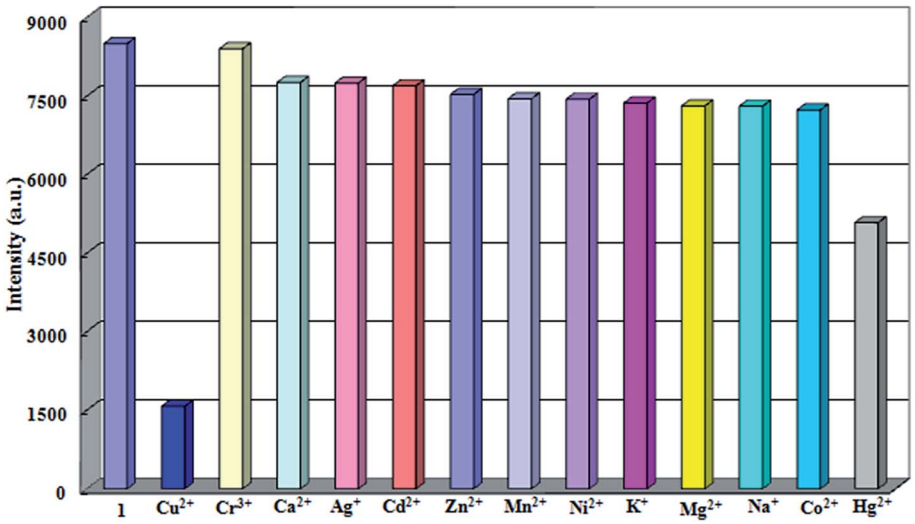

Fig. 3 Luminescence intensity of **1** after suspension in 1 M $M(NO_3)_x$ aqueous solution.

The luminescent behaviors of the H_3**L** ligand and compound **1** were tested (Fig. S4†). Upon excitation at 356 nm for H_3**L** and 366 nm for compound **1**, the MOF shows the resemblant emission peak with the organic ligand at about 420 nm, indicating that the luminescence of **1** is mainly based on the ligand-centered π–π* electronic transitions. Because of the good stability of **1** in both aqueous and DMF solution, it may be selected as the potential fluorescent materials (Fig. S2†).

3.4 Sensing of metal ions

For the purpose of studying sensing ability to different metal ions, **1** (18 mg) was grinded into the powder and suspended in 18 mL aqueous solution, sonicated for 30 min to ensure even dispersion. $M(NO_3)_x$ (1×10^{-3} M; M = Na^+, K^+, Ag^+, Mg^{2+}, Co^{2+}, Ca^{2+}, Ni^{2+}, Zn^{2+}, Cd^{2+}, Mn^{2+}, Cu^{2+}, Hg^{2+} and Cr^{3+}) was added into the aqueous suspension of **1** at room temperature, respectively. As shown in Fig. 3, Cu^{2+} ion exhibits an extremely significant quenching effect on the luminescence intensity, while Hg^{2+} ion shows a little degree of luminescence quenching, and almost no intensity change can be observed in the case of other metal ions, indicating **1** could detect Cu^{2+} ions through luminescence quenching. Further, the anti-interference experiments were investigated by introduction of Na^+, K^+, Ag^+, Mg^{2+}, Co^{2+}, Ca^{2+}, Ni^{2+}, Zn^{2+}, Cd^{2+}, Mn^{2+}, Hg^{2+} and Cr^{3+} into the system (Fig. 4). As a result, it indicated that **1** displayed the higher selectivity for Cu^{2+} ions among other metal ions.

To better understand the luminescence response of **1** to Cu^{2+} ions, the quantitative luminescence titration experiments were performed. The luminescence intensity of **1** gradually decreases with increasing concentration of Cu^{2+} ions (Fig. 5a). When the concentration of Cu^{2+} ions increases to 4×10^{-4} M, the

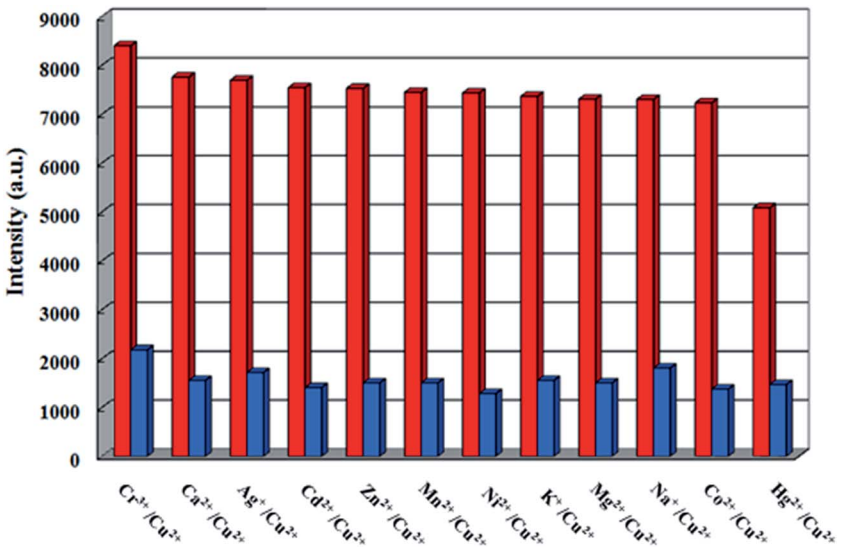

Fig. 4 Luminescence intensity of **1** in the presence of different metal ions (1 M, red: 1 + other metal ions, blue: 1 + other metal ions + Cu^{2+} ion).

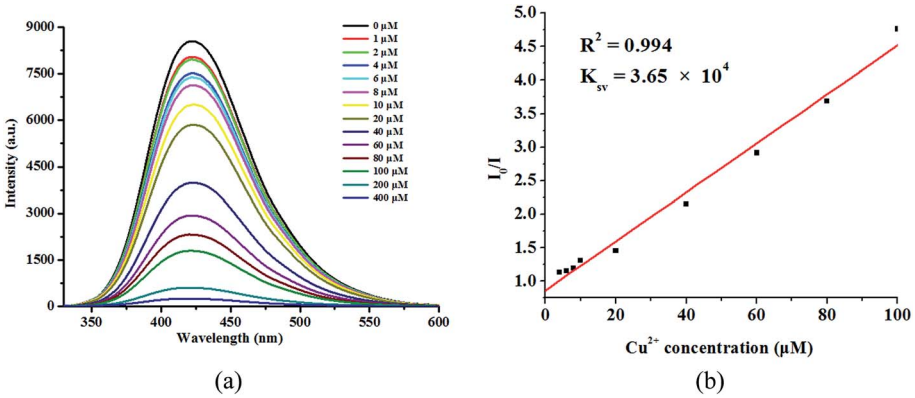

Fig. 5 View of (a) emission spectra of **1** in aqueous solutions with $Cu(NO_3)_2$ at different concentrations (λ_{ex} = 366 nm); (b) the relationship between the luminescence quenching efficiency (I_0/I) and the concentrations of Cu^{2+} ions.

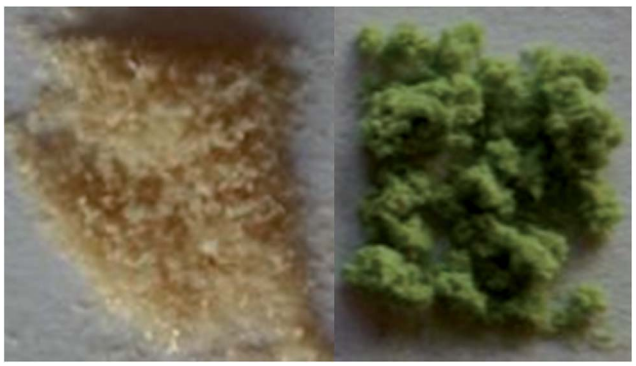

Fig. 6 Colors of **1** before (left) and after (right) soaked in aqueous solutions of $Cu(NO_3)_2$ (1 M).

quenching efficiency could almost reach 100%. Quantitatively, the quenching efficiency can be explained by the Stern–Volmer equation: $I_0/I = 1 + K_{sv}[M]$. The K_{sv} was calculated to be 3.65×10^4 M^{-1} (Fig. 5b), which is higher than some reported MOFs for Cu^{2+} ions sensing in aqueous solution.[35–37]

Moreover, compound **1** performed a significant color change, after it was soaked in the aqueous solution of $Cu(NO_3)_2$ with 10^{-3} M, indicating that it can be considered as a naked-eye detector for Cu^{2+} ions (Fig. 6), and the PXRD patterns of the product are in agreement with the simulated one (Fig. S5a†), showing that **1** keeps its original framework after soaking study. And the quenching mechanism can not be attributed to crystallographic alteration. As shown in Fig. 1a, the ions (Cd4 and Cd5) are located in six-coordinate environments. While, the coordination number of Cd^{2+} ion is usually more than six, the coordination polyhedrons are not stable and can be exchanged by other metal ions.[38,39] In addition, the significant color change of **1** reveals that Cu^{2+} ions may be incorporated into **1**. XPS (X-ray photoelectron spectroscopy) measurements were carried out to confirm the valency of copper in **1** and the peak at 932.58 eV can be considered to be $Cu2p_3$ spectra according to the former reports (Fig. S6†). The results suggest the presence of Cu^{2+} ions in Cd-MOF. Because of the unsaturated electronic state ($3d^9$) of Cu^{2+} ion, the excited electrons can transfer from the organic ligand (L^{3-}) to the empty d orbital of Cu^{2+} ions through the coordinate bonds. The transfer process hinders the photoluminescence and leading to the luminescence quenching phenomenon.[37] Moreover, the recyclable experiments (Fig. S7†) also indicate that Cd^{2+} ions of **1** may be partly exchanged by Cu^{2+} ions, because the luminescent intensity of **1**

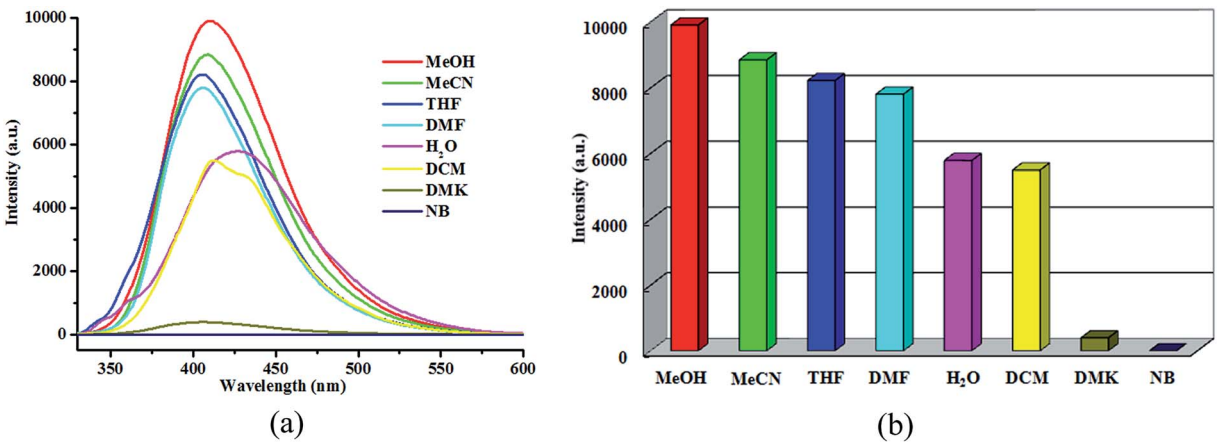

Fig. 7 View of (a) emission spectra of **1** in different organic solvents; (b) luminescence intensities of **1** in different organic solvents.

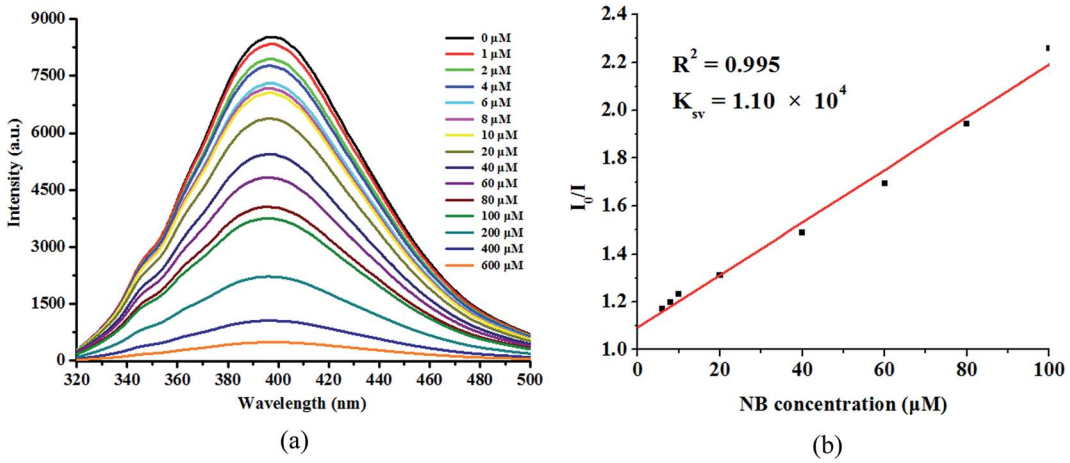

Fig. 8 View of (a) emission spectra of **1** at different concentrations of nitrobenzene (NB) in DMF; (b) the relationship between the luminescence quenching efficiency (I_0/I) and the concentrations of NB.

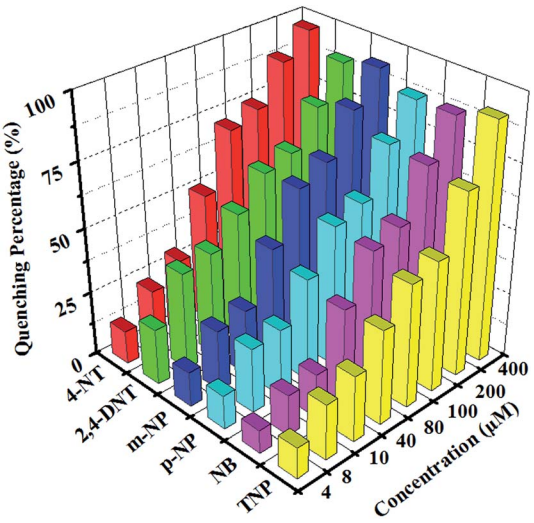

Fig. 9 Percentage of luminescence quenching obtained for different analytes at room temperature.

decreases after every run sensing. The high sensitivity and highly stability make **1** as a potential candidate for sensing Cu^{2+} ions in aqueous solution.

3.5 Sensing of nitroaromatic compounds

To investigate the sensitivity of **1** to small molecules, the luminescent intensities of some solvent suspensions were investigated. Several analyte molecules, such as acetonitrile (MeCN), *N*,*N*′-dimethyl formamide (DMF), tetrahydrofuran (THF), dichloromethane (DCM), acetone (DMK), methanol (MeOH), and nitrobenzene (NB) were selected. The emission spectra of different solvent suspensions have a degree of luminescence change upon excitation at 366 nm (Fig. 7). While NB exhibits the most effect quenching behavior for **1**, it turn out to be **1** can serve as the sensor for detecting NB.

The relationship between the luminescent intensities and the concentration of NB, was studied by gradual addition of NB to the DMF suspension of **1** (Fig. 8a). The luminescent intensity of **1** is quenched completely at the concentration of NB up to 6×10^{-4} M, indicating that compound **1** has a good detectability to NB, and can also keep its original structure (Fig. S5b†). The K_{sv} value for NB was calculated to be 1.10×10^4 M^{-1} (Fig. 8b). The good quenching effect of NB prompted us to further test other NACs. 4-NT, 2,4-DNT, *m*-NP, *p*-NP, and TNP were added to studied the corresponding emission responses (Fig. S8†). In S8, a new emission between 460–480 nm appeared when the concentration of TNP was added up to 200 μM, which could be attributed to either energy transfer from the excited donor or the direct excitation of the analyte.[40,41] The concentration of NACs is 60 μM, the fluorescence quenching efficiencies of 4-NT, 2,4-DNT, *m*-NP, *p*-NP, TNP and NB are 97%, 97%, 95%, 94%, 97%, 94%, respectively (Fig. 9). It shows that **1** can also be highly sensitive to identify a variety of NACs. Furthermore, compound **1** can be recycled by centrifuging the dispersed solution and washing several times by DMF. The quenching efficiencies for sensing TNP is basically unchanged up to three cycles, suggesting that **1** can also be a potential NACs fluorescent sensor (Fig. S9†).

The electron-rich π-conjugated ligand has a higher LUMO energy than the analytes (Table S3†). One possible quenching mechanism may be ascribed to the photo-induced electron transfer (PET) from an electron-rich excited MOF to the electron-deficient NACs.[42,43] But the order of quenching efficiency is not in accordance with the LUMO energies, which indicates that may exist other mechanisms. The absorption spectra of NACs and the emission spectrum of **1** have been carefully studied, the overlap between them usually results in the resonance energy transfer (RET) process, which also can cause the quenching of the fluorescence intensity (Fig. S10†).[44–46] Under the influence of two different mechanisms, all NACs show similar quenching efficiencies in the present research.

4. Conclusions

In summary, a new 3D luminescent Cd-MOF (**1**) was synthesized by solvothermal reaction. The compound can detect Cu^{2+} ions

and NACs sensitively through luminescence quenching method. Furthermore, it can be considered as a naked-eye detector for Cu^{2+} ions. And the structure of **1** remains stable after soaked in $Cu(NO_3)_2$ or NB solution. All the results suggest that **1** is a promising luminescent sensor for Cu^{2+} ions and NACs.

Conflicts of interest

There are no conflicts to declare.

Acknowledgements

This work was supported by the National Natural Science Foundation of China (21501041), the Natural Science Foundation of Hebei Province, China (B2017201094, B2017201131), the State Key Laboratory of Fine Chemicals (KF1501), and Postgraduate's Innovation Fund Project of Hebei Province (CXZZSS2017011).

References

1 L. Y. Pang, N. N. Bai, J. C. Jin, G. P. Yang, Y. L. Wu, X. J. Luan and Y. Y. Wang, *ChemistrySelect*, 2016, **1**, 3946–3953.
2 X. Zhang, Z. J. Wang, S. G. Chen, Z. Z. Shi, J. X. Chen and H. G. Zheng, *Dalton Trans.*, 2017, **46**, 2332–2338.
3 Y. Salinas, R. Martinez-Manez, M. D. Marcos, F. Sancenon, A. M. Castero, M. Parra and S. Gil, *Chem. Soc. Rev.*, 2012, **41**, 1261–1296.
4 A. Lan, K. Li, H. Wu, D. H. Olson, T. J. Emge, W. Ki, M. Hong and J. Li, *Angew. Chem., Int. Ed.*, 2009, **48**, 2334–2338.
5 G. L. Wang, J. J. Xu and H. Y. Chen, *Nanoscale*, 2010, **2**, 1112–1114.
6 C. Guo, P. Li, M. Pei and G. Zhang, *Sens. Actuators, B*, 2015, **221**, 1223–1228.
7 H. C. Zhou, M. Li, X. R. Lin, W. Chen, G. H. Chen, X. C. Huang and D. Li, *Angew. Chem., Int. Ed.*, 2015, **54**, 10454–10459.
8 J. W. Liu, L. F. Chen, H. Cui, J. Y. Zhang, L. Zhang and C. Y. Su, *Chem. Soc. Rev.*, 2014, **43**, 6011–6061.
9 C. Y. Sun, X. L. Wang, X. Zhang, C. Qin, P. Li, Z. M. Su, D. X. Zhu, G. G. Shan, K. Z. Shao, H. Wu and J. Li, *Nat. Commun.*, 2013, **4**, 2717–2725.
10 D. De, T. K. Pal, S. Neogi, S. Senthilkumar, D. Das, S. S. Gupta and P. K. Bharadwaj, *Chem.–Eur. J.*, 2016, **22**, 3387–3396.
11 P. P Bag, D. Wang, Z. Chen and R. Cao, *Chem. Commun.*, 2016, **52**, 3669–3672.
12 N. B. Nguyen, G. H. Dang, D. T. Le, T. Truong and N. T. S. Phan, *ChemPlusChem*, 2016, **81**, 361–369.
13 L. Wang, G. L. Fan, X. F. Xu, D. M. Chen, L. Wang, W. Shi and P. Cheng, *J. Mater. Chem. A*, 2017, **5**, 5541–5549.
14 Y. Cheng, J. Wu, C. Guo, X. G. Li, B. Ding and Y. Li, *J. Mater. Chem. B*, 2017, **5**, 2524–2535.
15 J. W. Ye, L. M. Zhao, R. F. Bogale, Y. Gao, X. X. Wang, X. M. Qian, S. Guo, J. Z. Zhao and G. L. Ning, *Chem.–Eur. J.*, 2015, **21**, 2029–2037.
16 W. P. Lustig, S. Mukherjee, N. D. Rudd, A. V. Desai, J. Li and S. K. Ghosh, *Chem. Soc. Rev.*, 2017, **46**, 3242–3285.
17 B. Wang, Q. Yang, C. Guo, Y. X. Sun, L. H. Xie and J. R. Li, *ACS Appl. Mater. Interfaces*, 2017, **9**, 10286–10295.
18 D. M. Chen, N. N. Zhang, C. S. Liu and M. Du, *J. Mater. Chem. C*, 2017, **5**, 2311–2317.
19 J. T. Guo, W. Z. Zeng, Q. F. Chen, L. P. Chen, Y. Yang, C. L. Cang, D. J. Ren and Y. X. Jiang, *Nature*, 2016, **531**, 249–252.
20 M. Chen, W. M. Xu, J. Y. Tian, H. Cui, J. X. Zhang, C. S. Liu and M. Du, *J. Mater. Chem. C*, 2017, **5**, 2015–2021.
21 H. J. Feng, L. Xua, B. Liuc and H. Jiao, *Dalton Trans.*, 2016, **45**, 17392–17400.
22 J. Sahoo, S. B. Waghmode, P. S. Subramanian and M. Albrecht, *ChemistrySelect*, 2016, **1**, 1943–1948.
23 J. Dong, H. Xu, S. L. Hou, Z. L. Wu and B. Zhao, *Inorg. Chem.*, 2017, **56**, 6244–6250.
24 X. X. Li, H. Y. Xu, F. Z. Kong and R. H. Wang, *Angew. Chem., Int. Ed.*, 2013, **125**, 14014–21401.
25 C. Q. Zhang, Y. Yan, Q. H. Pan, L. B. Sun, H. M. He, Y. L. Liu, Z. Q. Liang and J. Y. Li, *Dalton Trans.*, 2015, **44**, 13340–13346.
26 Y. Y. Jiang, L. B. Sun, J. F. Du, Y. C. Liu, H. Z. Shi, Z. Q. Liang and J. Y. Li, *Cryst. Growth Des.*, 2017, **17**, 2090–2096.
27 C. H. Zhang, L. B. Sun, Y. Yan, Y. C. Liu, Z. Q. Liang, Y. L. Liu and J. Y. Li, *J. Mater. Chem. C*, 2017, **5**, 2084–2089.
28 D. Wang, L. B. Sun, C. Q. Hao, Y. Yan and Z. Q. Liang, *RSC Adv.*, 2016, **6**, 57828–57834.
29 L. H. Cao, F. Shi, W. M. Zhang, S. Q. Zang and T. C. W. Mak, *Chem.–Eur. J.*, 2015, **21**, 15705–15712.
30 X. X. Jia, R. X. Yao, F. Q. Zhang and X. M. Zhang, *Inorg. Chem.*, 2017, **56**, 2690–2696.
31 Y. L. Wu, G. P. Yang, Y. Q. Zhao, W. P. Wu, B. Liu and Y. Y. Wang, *Dalton Trans.*, 2015, **44**, 3271–3277.
32 Bruker AXS, *SAINT Software Reference Manual*, Madison, WI, 1998.
33 G. M. Sheldrick, *Acta Crystallogr., Sect. A: Found. Crystallogr.*, 2008, **64**, 112.
34 B. Gole, A. K. Bar and P. S. Mukherjee, *Chem. Commun.*, 2011, **47**, 12137–12139.
35 T. T. Zheng, J. Zhao, Z. W. Fang, M. T. Li, C. Y. Sun, X. Li, X. L. Wang and Z. M. Su, *Dalton Trans.*, 2017, **46**, 2456–2461.
36 Y. Xiao, Y. Cui, Q. Zheng, S. Xiang, G. Qian and B. Chen, *Chem. Commun.*, 2010, **46**, 5503–5505.
37 Z. M. Zhou, W. Shi, H. M. Li, H. Li and P. Cheng, *J. Phys. Chem. C*, 2014, **118**, 416–426.
38 Z. Zhang, L. Wojtas, M. Eddaoudi and M. J. Zaworotko, *J. Am. Chem. Soc.*, 2013, **135**, 5982–5985.
39 Z. Zhang, L. Zhang, L. Wojtas, P. Nugent, M. Eddaoudi and M. J. Zaworotko, *J. Am. Chem. Soc.*, 2012, **134**, 924–927.
40 K. S. Asha, K. Bhattacharyya and S. Mandal, *J. Mater. Chem. C*, 2014, **2**, 10073–10081.
41 S. Ramanchandran, Z. D. Popovic, K. S. Schuermann, F. Cucinotta, G. Calzaferri and L. D. Cola, *Small*, 2011, **7**, 1488–1494.
42 G. Y. Wang, L. L. Yang, Y. Li, H. Song, W. J. Ruan, Z. Chang and X. H. Bu, *Dalton Trans.*, 2013, **42**, 12865–12868.

43 H. Sohn, M. J. Sailor, D. Magde and W. C. Trogler, *J. Am. Chem. Soc.*, 2003, **125**, 3821–3830.
44 D. Banerjee, Z. C. Hu and J. Li, *Dalton Trans.*, 2014, **43**, 10668–10685.
45 Z. C. Hu, B. J. Deibert and J. Li, *Chem. Soc. Rev.*, 2014, **43**, 5815–5840.
46 L. L. Zhang, Z. X. Kang, X. L. Xin and D. F. Sun, *CrystEngComm*, 2016, **18**, 193–206.